TÜBİTAK

Turkish Journal of Engineering & Environmental Sciences

http://journals.tubitak.gov.tr/engineering/

Research Article

Turkish J Eng Env Sci
(2014) 38: 354 – 362

doi:10.3906/muh-1501-11

Velocity measurements of a free-surface turbulent flow over smooth and rough beds

Akram ABBASPOUR*, Davood FARSADIZADEH
Department of Water Engineering, University of Tabriz, Tabriz, Iran

Received: 19.01.2015 • **Accepted/Published Online:** 09.08.2015 • **Printed:** 04.03.2016

Abstract: The effect of different types of surface roughness on a turbulent boundary layer was studied using 1D velocity measurements in a relatively high Reynolds flow. The roughness consisted of trapezoidal ribs with horizontal spacing and roughness height k. The roughness elements were aligned in a direction transverse to the flow. A series of 7 tests of fully rough turbulent subcritical flow over two-dimensional transverse repeated trapezoidal ribs was undertaken, in which the ribs were varied to give uniform rib spacing-to-height ratios of p/k = 6–36. Measurements of the velocity were carried out over a range of Reynolds numbers, 81735 < Re < 144,110. The results show that the mean profiles of all the surfaces collapse well in the velocity defect form.

Key words: Roughness function ΔU^+, trapezoidal rib roughness, turbulence, velocity profile

1. Introduction

Perry et al. [1] divided wall roughness into two types depending on the apparent length scale influencing the flow. Simpson [2] proposed d-type and k-type roughnesses occurring for p/k < 5 and p/k > 5, respectively, where p is crest-to-crest rib spacing (Figure 1). Jimenez [3] suggested d-type roughness to occur for closely spaced two-dimensional ribs of p/k < 4–5, with k-type roughness occurring for larger rib spacing. The studies by Nikuradse [4] and Perry et al. [1] showed that the rough-wall boundary condition affects the mean velocity distribution in the inner region. In the experimental measurements of Nikuradse [4] on rough beds, intensive efforts were focused on practical engineering applications of this research, such as drag reduction.

Bisceglia et al. [5] studied the effect of two different types of bed roughness on a turbulent boundary layer using 2-component LDV measurements in a relatively high-speed water tunnel. One roughness consisted of square ribs at a horizontal spacing p equal to 2k. The other consisted of cylindrical rods with p/k equal to 4. Both roughness elements were aligned in a direction transverse to the flow.

Coleman et al. [6] studied fully rough turbulent subcritical flow over two-dimensional transverse repeated-rib roughnesses of varying spacing p/k = 1–16 (roughness spacing/height ratio), with k/H = 0.09. The experimentally determined momentum balance, including the effects of secondary currents and flow acceleration, was found to agree well with theoretical expectations. Application of the double-averaging methodology to open channel flows over rough beds was done by Nikora et al. [7]. Guo and Julien [8] and Guo et al. [9] proposed a modified log-wake law that well represents experimental data in pipes and a zero-pressure gradient boundary layer. Nikora et al. [10] promoted the concept of the double-averaged hydrodynamic equations and identified

*Correspondence: akabbaspour@yahoo.com

four distinct flow types depending on their relative submergence. The above flow subdivision and flow types represent a useful schematization that may help in developing relationships for the vertical distribution of flow characteristics. Guo and Julien [11] suggested that the modified log-wake law, which was developed for turbulent boundary layers and pipe flows, be extended to turbulent flows in open channels. Volino et al. [12] investigated turbulence measurements over a two-dimensional roughness and compared them to previous results from a smooth wall. The two-dimensional bars led to significant changes in the turbulence in the outer flow. Reynolds stresses increased, although the mean flow was not as significantly affected.

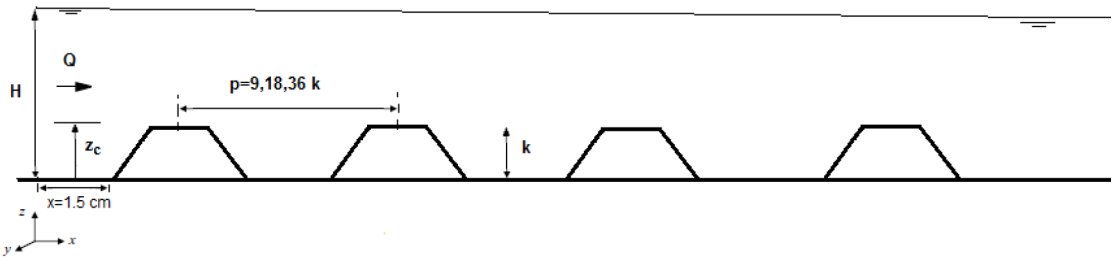

Figure 1. Roughness element geometry and streamwise spacing for trapezoidal rib roughness.

Direct numerical simulation (DNS) of a spatially developing turbulent boundary layer (TBL) over repeated-rib roughness was performed by Lee et al. [13] to investigate the effects of 3D bed roughness on the properties of the TBL. The characteristics of the TBL over the 3D cube-roughened bed were compared with the results of a DNS of the TBL over a 2D rib-roughened bed. The effect of depth on turbulent open channel flow past a train of rib elements was examined by Roussinova and Balachandar [14]. The experiments were conducted in the fully rough regime to document the turbulence characteristics of the flow at two different rib spacings p/k of 9 and 18.

Recognizing the lack of focus to date on flow details over two-dimensional trapezoidal repeated-rib roughness, a series of experiments were thereby undertaken to assess the variation with rib spacing of p/k = 6–36 of the overlying flow structure and dynamics, with a principal focus on velocity and skin-friction coefficients. In this study, a new law is proposed for the velocity profile in the outer region of a channel. The following section details averaging measures central to understanding flow over heterogeneous bed roughness. Parameterization of the rough-wall velocity profile is then outlined, the experiments undertaken are described, and the results and implications of the study are presented. The outer layers of turbulent boundary layers and turbulent channel flows react differently in response to surface roughness compared to a cube-roughened bed.

2. Materials and methods

The experiments were conducted in a metal-glass sided flume with a rectangular cross-section. The flume was 0.25 m wide, 0.5 m deep and 10 m long. The slope of the channel was 0.002. The discharge was measured by a triangular weir placed at the end. The water depths were measured using a point gauge, with the least reading of 0.1 mm installed on a rail along the flume.

The rough bed was established using a 25-mm-long roughness strip with trapezoidal rib of height k = 10, 15 mm. The top side lengths of the trapezoidal ribs were 10 and 15 mm. The length of the test section was approximately 1.5 m. Each trapezoidal rib roughness (height k) was attached to one of the test section walls with distance p along the flume. The values of the experimental parameters investigated were p/k = 6,

9, 12, 18, 24, 36. Figure 1 shows the geometry and horizontal spacing for the trapezoidal rib roughness. The experimental tests were conducted on a smooth bed for establishing data to assess the effects of rib roughness.

The ratio $H/\mathrm{k} = 6.8$–10.4 defines the studied flow as the flow of intermediate submergence (H = mean flow depth; k = roughness height), as suggested by Nikora et al. [7].

The u velocity was measured using a micropropeller velocity meter at 4–10 mm vertical spacings focused near the rib and 30–100 mm horizontal spacings (increasing with bar spacing).

Table 1 summarizes hydraulic parameters for the tests, where Froude number $\mathrm{Fr}_1 = \mathrm{u}_m/(gH)^{0.5}$, Reynolds number $\mathrm{Re} = 4\mathrm{Ru}_m/\nu$, R = hydraulic radius, and shear velocity was determined from the hydraulic radius and the measured free-surface slope, $u_* = (gRS_w)^{0.5}$. All tests were fully rough flow of the roughness Reynolds number, $\mathrm{k}^+ = \mathrm{k}u_*/\nu > 70$.

Table 1. Test hydraulic parameters.

Beds	p/k	H (m)	K (mm)	u_m (m/s)	Re	Fr_1	u_* (m/s)	S_W ($\times 10^3$)
Smooth	0	0.104	0	0.67	144,110	0.81	0.023	1
Trapezoidal (1)	9	0.1	10	0.48	98790	0.7	0.023	1
	18	0.104	10	0.51	109700	0.7	0.094	15
	36	0.102	10	0.53	113000	0.72	0.098	17
Trapezoidal (2)	6	0.103	15	0.44	81735	0.62	0.075	11
	12	0.104	15	0.48	90340	0.64	0.061	8
	24	0.104	15	0.49	96790	0.66	0.06	7.8

3. Results and discussion

The flow characteristics over the two rough beds and the smooth bed are shown in Table 1.

3.1. Velocity profiles

The mean streamwise velocity profiles normalized with bed shear velocity u_* are presented.

Figure 2 shows velocity distributions for forward flow for a smooth bed. Figure 2 indicates that the values of $u^+ = u/u_*$ are higher for smooth beds.

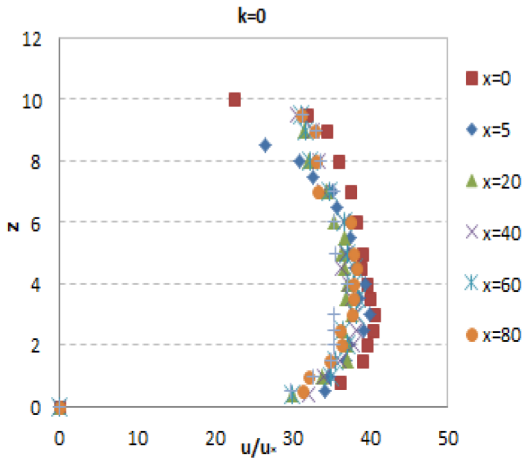

Figure 2. Velocity profiles over a smooth bed (legend values are distance x).

To examine the effect of roughness on mean flow, the velocity profiles of three cases with different p/k are selected, which are shown in Figures 3 and 4.

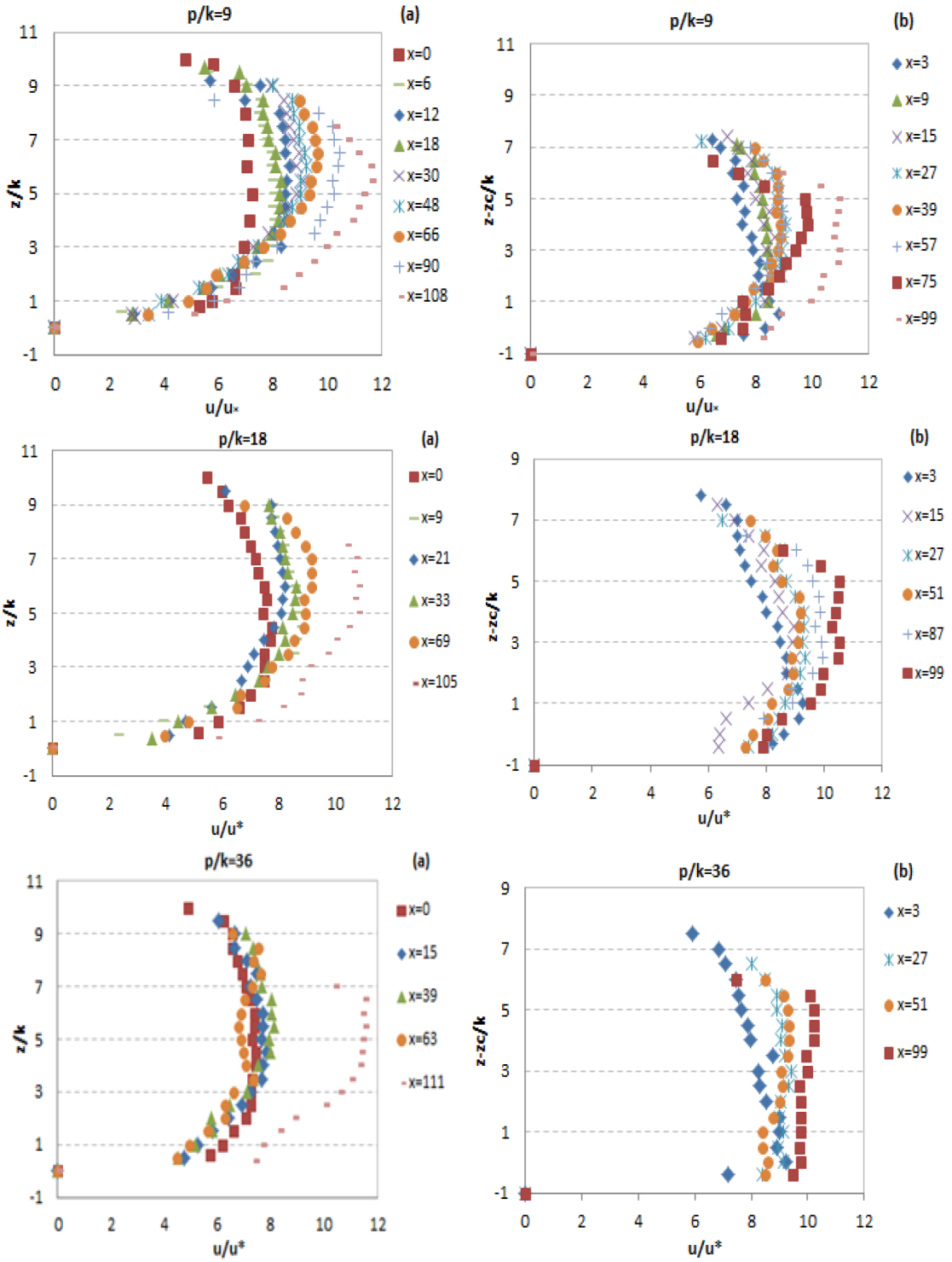

Figure 3. Velocity profiles (a) inside cavities and (b) over trapezoidal ribs' top for k = 1 cm (legend values are distance x).

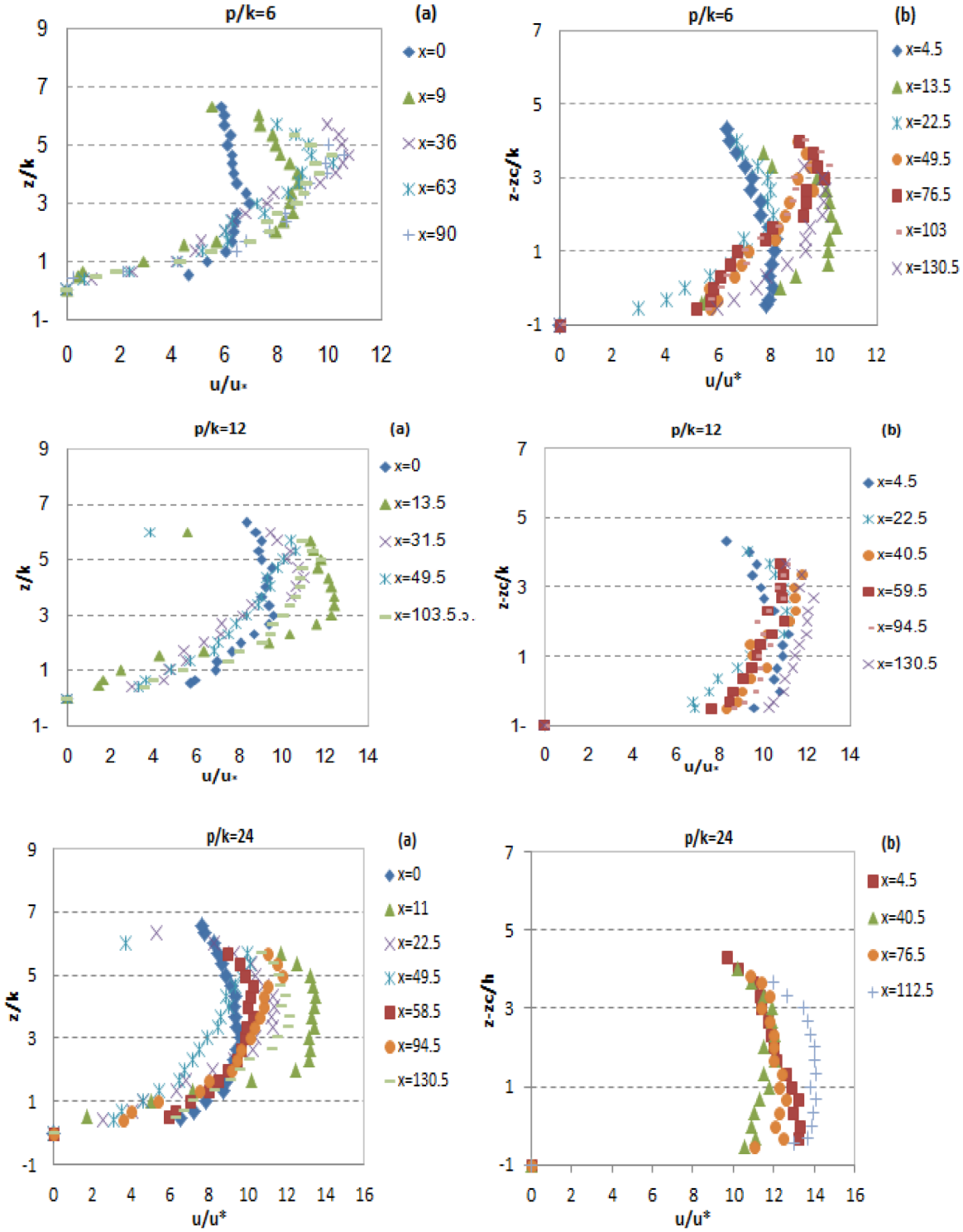

Figure 4. Velocity profiles (a) inside cavities and (b) over trapezoidal ribs' top for k = 1.5 cm (legend values are distance x).

Figures 3 and 4 demonstrate the streamwise velocity profiles for which point measurements are available. These locations are inside the cavity (a) and above the top of a bar (b).

In the outer region, the velocity profiles can be estimated from the following equation:

$$\kappa \frac{u}{u_*} = \frac{1}{-} Ln \frac{u_* z}{\nu} + B - \Delta U^+, \tag{1}$$

where κ and B are 0.41 and 5, respectively, the normalized effective height $y^+ = \frac{u_* z}{\nu}$, and ΔU^+ represents the roughness-caused shift. For a smooth wall, ΔU^+ is zero.

The mean velocity profiles for all the test surfaces are presented in Figure 5 and 6. The mean velocity is normalized by the local shear velocity at each position. The smooth bed results collapse on a smooth log-law profile [12], while the rough bed results display a log region that is shifted by ΔU^+ below the smooth bed profile. It can be seen that for vertical distances far from the rough bed the velocity distribution departs from the log-law. This is partly caused by air friction near the water surface. The departure of the velocity profile of the log-law due to roughness is corrected by the roughness function ΔU^+.

As expected from the form of Eq. (1), the vertical distribution of velocities of flow over roughness-topped beds displays a logarithmic behavior (Figure 6). Owing to the higher surface drag, the flow rate is reduced and the mean velocity profile on the rough bed is less bodied than that obtained on a smooth bed (Figure 5).

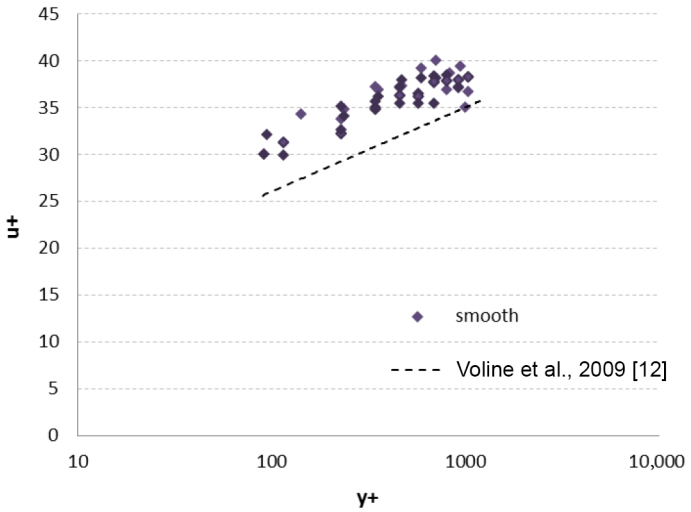

Figure 5. Mean streamwise velocity profiles in smooth bed.

The variation in ΔU^+ in Table 2 reflects the relative shift of the logarithmic profile from that for a smooth wall. In Table 2, the normalized velocities show a much larger shift for the trapezoidal roughness ΔU^+ with different *pvk* compared to a smooth bed. The maximum values of ΔU^+ occur for a trapezoidal rib roughened channel with k = 1.5 cm for smaller $pvk = 6$. There is no sufficient evidence to suggest that ΔU^+ can vary as a function y^+ with a different slope.

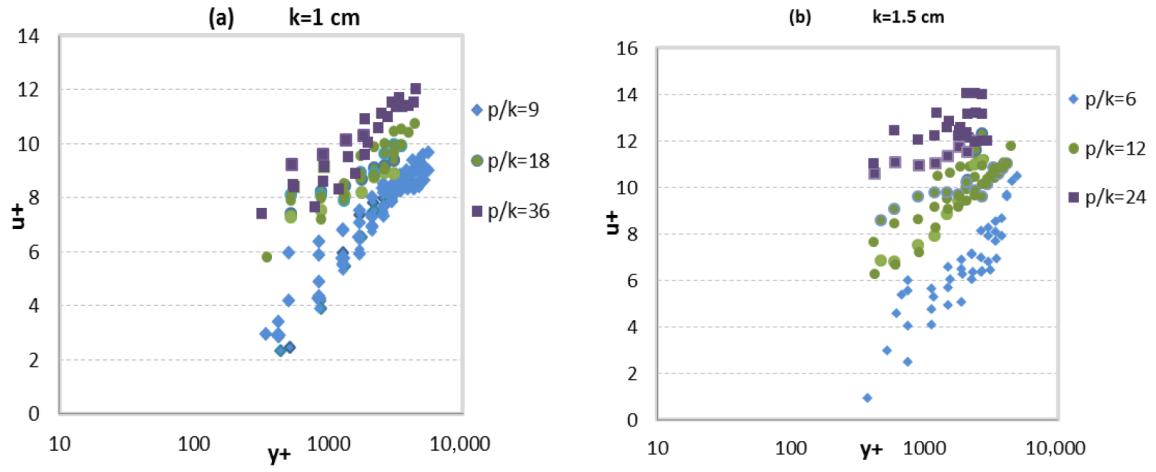

Figure 6. Mean streamwise velocity profiles in trapezoidal rib roughened channel with (a) k = 1.5 cm and (b) k = 1 cm.

Table 2. Boundary layer parameters for the test cases.

Surface	p/k	k^+	ΔU^+	C_f	F_t
Smooth	0	0	0	0.002	0.01
Trapezoidal (1)	9	820	+17	0.057	0.26
	18	864	+15	0.052	0.25
	36	887	+16	0.05	0.24
Trapezoidal (2)	6	1061	+18	0.062	0.26
	12	904	+17	0.034	0.14
	24	894	+14.5	0.03	0.12

As expected, the rough profiles are shifted downwards with the amount equivalent to the roughness function (ΔU^+), which was obtained directly from mean velocity profiles. The downward shift of ΔU^+ for p/k = 9 is greater ($\Delta U^+ = 17$, k = 10 mm) than the result obtained by Roussinova and Balachandar [14] (p/k = 9, $\Delta U^+ = 14.8$, k = 10 mm) in rib elements, but the downward shift of ΔU^+ for p/k = 18 ($\Delta U^+ = 15$, k = 10 mm) is close to the result obtained by Roussinova and Balachandar [14] (p/k = 18, $\Delta U^+ = 14.8$, k = 10 mm).

In a roughened channel, however, both form drag and skin friction contribute to the flow resistance. Since the mean flow varies periodically with x in the present configuration, so does the shear stress, τ.

The skin friction coefficient, $C_f = 2[u_*/U_1]^2$, where U_1 = mean velocity upstream, is also shown in Table 2. For the trapezoidal roughness, C_f is approximately independent of the Reynolds number when $Re > 10^4$. The skin friction coefficient C_f decreased with increasing rib spacing.

Figures 7 and 8 show the variations of the skin friction coefficient along the roughened wall. The skin friction coefficient decreases along the streamwise distance. The friction coefficient fluctuated for p/k = 36 due to water depth changes.

The friction factor values, $F_t = 8[u_*/U_1]^2$, in Table 2 indicate that a maximum drag due to bed roughness occurs at p/k = 9 for k = 1 cm and p/k = 6 for k = 1.5. The computed wall drag indicates similar trends in flow resistance, with maximum flow resistance confirmed to occur for a smaller p/k.

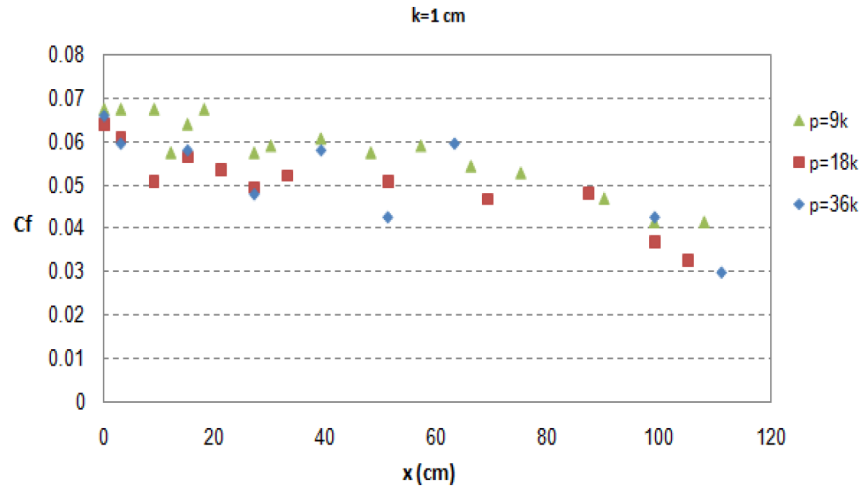

Figure 7. The streamwise variation of the skin-friction coefficient C_f for k = 1.

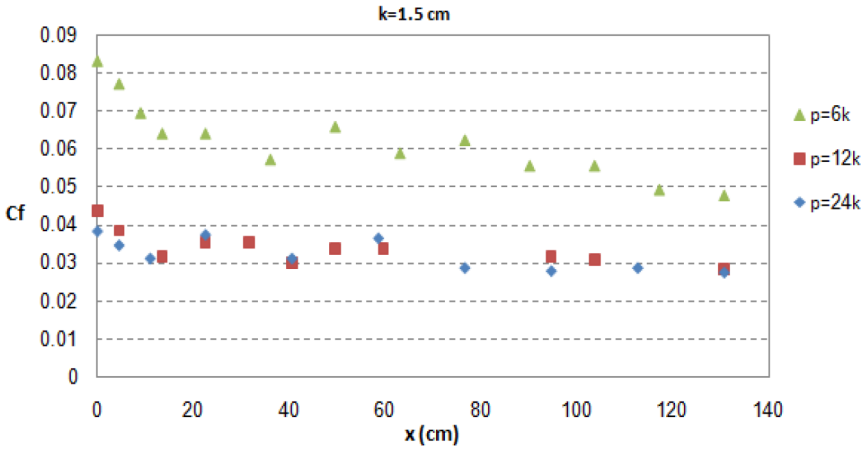

Figure 8. The streamwise variation of the skin-friction coefficient C_f for k = 1.5.

4. Conclusions

In this work, the mean velocities of two rough beds were compared to that for a smooth bed. The velocity measurements carried out in the turbulent boundary layer at large Reynolds numbers over two rough beds and a smooth bed showed that the turbulent field throughout most of the boundary layer differed among the three wall beds.

The roughness function ΔU^+, the characteristic downward shift of the logarithmic part of the mean velocity profile, was found to be more than 14.5. For both rough beds, ΔU^+ scales logarithmically with $y+$. Over a trapezoidal roughness with p/k = 6 (k = 1.5 cm), the parameter $\Delta U^+ \approx 19$ is considerably greater for the trapezoidal rib roughness than for the rough bed. In the smooth bed the log-low hold region is commonly considered as $30 < y^+ < 1000$, while it ranges from 300 to 1500 in different types of rough beds. Coleman et al. [6] computed skin-friction coefficient C_f about 0.032 and 0.029 for p/k = 8 and p/k = 16 respectively with cube rib roughness (k = 1 cm) and these values are less than the skin-friction coefficient C_f of 0.057 and 0.052 for the trapezoidal roughness with p/k = 9 and 18 (k = 1 cm). Thus, skin-friction coefficient C_f is greater for trapezoidal rib roughness than repeated-rib roughness.

Acknowledgment

This study was supported by the Research Affairs Unit of Tabriz University under Project No. 27/1631-1.

5. Notation

B	logarithmic profile additive constant
C_f	wall skin friction coefficient
Fr_1	Froude number, $Fr_1 = u_m/(gH)^{0.5}$
F_t	friction factor, $F_t = 8[u_*/U_1]^2$
g	gravitational acceleration
H	upstream mean flow depth
k	roughness height
k^+	roughness Reynolds number, $k^+ = ku_*/\nu$
p	crest-to-crest spacing
R	hydraulic radius, $R = (bH)\ /\ (b+2H)$
Re	Reynolds number, $Re = 4Ru_m/\nu$
S_w	water surface slope
u_m	mean velocity
u_*	shear velocity, $u_* = (gRS_w)^{0.5}$
y^+	the normalized effective height, $y^+ = \frac{u_* z}{\nu}$
z	elevation above the between-rib cavity base
z_c	rib crest elevation
κ	von Karman's constant, k = 0.4–0.42
ν	fluid kinematic viscosity
τ	wall shear stress

References

[1] Perry AE, Schofield WH, Joubert PN. Rough wall turbulent boundary layers. J Fluid Mech 1969; 37: 383–413.

[2] Simpson RL. A generalized correlation of roughness density effects on the turbulent boundary layer. AIAA J 1973; 11: 242–244.

[3] Jimenez J. Turbulent flow over rough walls. Ann Rev Fluid Mech 2004, 36: 173–196.

[4] Nikuradse J. Laws of Flows in Rough Pipes, VDI Forschungsheft 361, NACA Technical Memorandum 1292. Berlin, Germany: Verein Deutscher Ingenieure, 1933.

[5] Bisceglia S, Smalley RJ, Djenidi L, Antonia RA. Structure of rough wall turbulent boundary layers at relatively high Reynolds number. In: 14th Australasian Fluid Mechanics Conference; 2001; Adelaide, Australia. pp. 195–198.

[6] Coleman SE, Nikora VR, McLean SR, Schlicke E. Spatially averaged turbulent flow over square ribs. J Eng Mech-ASCE 2007; 133: 194–204.

[7] Nikora V, Koll K, McEwan I, McLean S, Dittrich A. Velocity distribution in the roughness layer of rough-bed flows. J Hydraul Eng-ASCE 2004; 130: 1036–1042.

[8] Guo J, Julien PY. Modified log-wake law for turbulent flow in smooth pipes. J Hydraul Res 2003; 41: 493–501.

[9] Guo J, Julien PY, Meroney RN. Modified log-wake law for zero-pressure-gradient turbulent boundary layers. J Hydraul Res 2005; 43: 421–430.

[10] Nikora V, McEwan I, McLean S, Coleman SE, Pokrajac D, Walters R. Double-averaging concept for rough-bed open-channel and overland flows: theoretical background. J Hydraul Eng-ASCE 2007; 133: 873–883.

[11] Guo J, Julien PY. Application of the modified log-wake law in open-channels. Journal of Applied Fluid Mechanics 2008; 1: 17–23.

[12] Volino RJ, Schultz MP, Flack KA. Turbulence structure in a boundary layer with two-dimensional roughness. J Fluid Mech 2009; 635: 75–101.

[13] Lee JA, Sung HJ, Krogstad PA. Direct numerical simulation of the turbulent boundary layer over a cube-roughened wall. J Fluid Mech 2011; 669: 397–431.

[14] Roussinova V, Balachandar R. Open channel flow past a train of rib roughness. J Turbul 2011; 12: 1–17.